Chemical Engineering Journal 158 (2010) 296–304

Contents lists available at ScienceDirect

Chemical Engineering Journal

journal homepage: www.elsevier.com/locate/cej

Mapping of cavitational activity in high frequency sonochemical reactor

Vinayak S. Sutkar, Parag R. Gogate*

Chemical Engineering Department, Institute of Chemical Technology, Matunga, Mumbai 40019, India

ARTICLE INFO

Article history:
Received 20 August 2009
Received in revised form 12 January 2010
Accepted 25 January 2010

Keywords:
Acoustic cavitation
Cavitational activity
Mapping
Wave equation
Sonochemical reactor

ABSTRACT

In the present work, distribution of cavitational activity in high frequency sonochemical reactor has been quantified with the help of different mapping techniques based on experimental investigations and theoretical analysis. In experimental investigations, amount of iodine liberation at different locations has been quantified whereas quantification of cavitational activity using theoretical analysis is based on the solution of space dependent part of the wave equation with the help of COMSOL Multi-physics software. The effect of frequencies of irradiation with and without presence of electrolyte solution (NaCl) to intensify the cavitational activity has been investigated in order to understand behavior of cavitation phenomena. The analysis presented in the work helps in identifying the regions with maximum cavitational intensity so as to obtain maximum efficacy for the desired physical or chemical transformations.

1. Introduction

The use of ultrasound induced acoustic cavitation as source of energy for intensification of physical and chemical processing applications has been well established on laboratory scale of operation [1–2]. Some of the applications of cavitational reactors reported in the literature [3–4] are chemical synthesis, green chemistry, biotechnology, polymer chemistry, wastewater treatment, etc. However, it should be noted that in spite of extensive research and vital potential applications proven on laboratory scale, there are limited number of chemical processing applications being carried out on an industrial scale, mainly attributed to the lack of suitable reactor design and scale-up strategies to transform the successful laboratory scale processes. The major problems identified in scale up of sonochemical reactors are local existences of cavitational events very near to irradiating surface, wide variation in energy dissipation rates in bulk of liquid and possible erosion of the sonicator surface at the high power intensities [1,5]. One step towards developing efficient design methodology for sonochemical reactors and finally achieve the goal of industrial scale operation is to develop pilot scale reactors and understand the spatial distribution of cavitational activity in the reactor using mapping. Mapping of sonochemical reactor is a stepwise procedure where cavitational activity can be quantified by means of primary effects (temperature or pressure measurement at the time of bubble collapse) and/or secondary effects (quantification of chemical or physical effects in terms of measurable quantities after the bubble collapse) to identify the active and passive zones. Most of previous studies related to mapping of sonochemical reactors are limited to laboratory scale operation [5,6]. The present work deals with mapping of a pilot scale reactor operating at higher frequencies (>100 kHz). The quantitative determination of cavitational activity has been carried out in terms of secondary as well as primary effects generated due to the cavitational collapse. The present work also reports studies using NaCl as an additive to alter the physicochemical properties of the liquid medium and establish the effect on the actual power dissipation in the liquid medium and the cavitational activity distribution. NaCl has been chosen as the model salt as it has been shown to intensify cavitationally induced transformations [7,8].

2. Materials and methods

2.1. Quantification of physicochemical properties of aqueous NaCl solution

The concentration of NaCl was varied over a range of 1–10% by weight. The selected range of concentrations was to cover all possible applications including wastewater treatment where higher concentrations are recommended as the role of NaCl is to selectively transfer the pollutant species at the site of cavitational collapse, in addition to altering the physicochemical properties of the liquid medium. The measurements of density, viscosity and surface tension have been carried out at room temperature with the help of specific gravity bottle, Ostwall viscometer and Kruss tensiometer which considered plate method and the obtained results are shown in Table 1. All measurements for quantification of physicochemical properties were repeated for five times and average values have been reported.

* Corresponding author. Tel.: +91 22 24145616; fax: +91 22 24145614.
E-mail address: pr.gogate@ictmumbai.edu.in (P.R. Gogate).

1385-8947/$ – see front matter © 2010 Elsevier B.V. All rights reserved.
doi:10.1016/j.cej.2010.01.051

Table 1
Physicochemical properties of NaCl solution.

Sr. No.	Concentration of NaCl solution % (w/v)	Density (kg/m^3)	Viscosity (cP)	Surface tension (mN/m)
1	0 (water)	997	1	71.50
2	1	1002	1.04	70.42
3	5	1022.46	1.15	70.01
4	10	1037.32	1.31	69.79

2.2. Experimental setup

Experiments were performed in a sonochemical reactor procured from Roop Telesonic Ltd., Mumbai and the schematic representation of the system has been given in Fig. 1. The reactor has a total operating capacity as 3.5 l with multiple driving frequencies of 694 and 204 kHz and maximum power rating of 55 and 224 W respectively. The internal dimensions of the reactor were, length = 24 cm, width = 14 cm and height = 14.5 cm. The reactor is fitted with two transducers of diameter 5 cm, located at bottom ($z = 0$) of reactor at (7, 7) and (17, 7) as shown in Fig. 1.

The wavelength of sound in water is found to be 0.216 and 0.735 cm for operating frequency of 694 and 204 kHz respectively (by assuming speed of sound as 1500 m/s). For investigations of cavitational activity, the reactor was divided into five planes (along z-direction) from bottom of the reactor at height corresponding to $10\lambda_1$, $20\lambda_1$, $30\lambda_1$, $40\lambda_1$ and $50\lambda_1$; where λ_1 is the wavelength for the frequency 694 kHz. The exact distance from bottom is 2.16, 4.32, 6.48, 8.64 and 10.8 cm where this distance also approximately corresponds to $3\lambda_2$, $6\lambda_2$, $9\lambda_2$, $12\lambda_2$ and 15 λ_2, where λ_2 is wavelength for frequency 204 kHz. The obtained plane was again subdivided at equal distance of 4 cm along length (locations at 4, 8, 12, 16, 20 cm) and 2 cm along width (locations at 2, 4, 6, 8, 10, 12 cm) which is shown in Fig. 1. Total 150 points were selected for investigations, 30 on each plane.

2.3. Calorimetric power measurements

The amount of energy actually dissipated in the bulk of liquid was estimated using calorimetric studies [9] and energy efficiency, which is the ratio of dissipated energy to the supplied electric energy has been estimated using following equations:

$$Q = mC_p\Delta T \quad (1)$$

$$\text{Calorimetric efficiency} = \frac{\text{Amount of energy gained by water}}{\text{Electrical energy input}} = \frac{mC_p\Delta T}{Et} \quad (2)$$

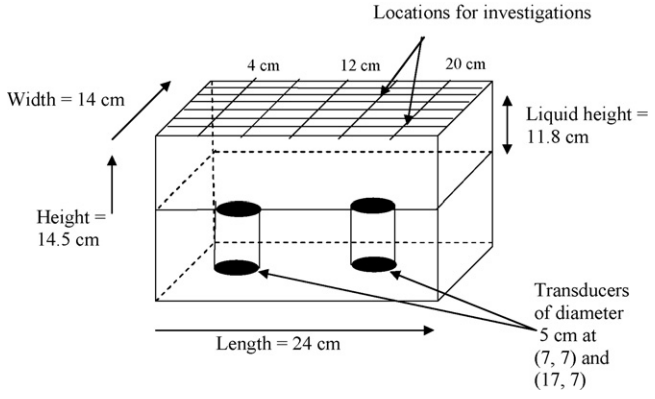

Fig. 1. Schematic view of sonochemical reactor and different locations for measurements.

where, m is mass of liquid (kg), C_p is specific heat capacity (J/kg K), ΔT is change in temperature in (K), E is electric energy supplied (W) for the time interval of t (s).

Measurements were performed by varying amount of liquid (maximum capacity being 3.5 l) to get optimum operating volume with maximum power dissipation rate.

2.4. Quantification of cavitational activity using Weissler reaction

In order to quantify the cavitational activity (secondary effects), decomposition of potassium iodide (KI) which is also known as Weissler reaction has been considered as model reaction. The reaction has been generally used as a measure to quantify the cavitational effects in sonochemical reactors [5,10–11]. When aqueous solution of potassium iodide (KI) is irradiated with ultrasound, decomposition of KI takes place and I^- ions are oxidized to give I_2^-. The excess I^- ions present in solution react with I_2 to form I_3^-. The different reactions taking place can be given as follows:

$$H_2O \rightarrow H^\bullet + OH^\bullet$$

$$OH^\bullet + I^- \rightarrow OH^- + I$$

$$I + I^- \rightarrow I_2^-$$

$$2I_2^- \rightarrow I_2 + 2I^-$$

$$I_2 + I^- \rightarrow I_3^-$$

The reaction was carried out at different locations as depicted in Fig. 1, with and without presence of NaCl for two frequencies of irradiations. For this purpose, 5 ml of 2% (w/v) KI solution was taken in small test tube (of outer diameter of 1.5 cm and height of approximately 15 cm). Same test tube was used every time to avoid the variation in attenuation of sound wave due to possible variation in the dimensions of different test tubes [5]. The analysis of amount of I_3^- ions formed during the decomposition reaction was performed using UV Spectrophotometer in the range of 352–354 nm wavelength. The same procedure was repeated for all the locations using same test tube for three times and an average value of iodine has been reported.

2.5. Quantification of local pressure field by wave equation

Quantification of pressure amplitude at different planes in the reactor has been carried out by solving space dependent part of wave equation (Helmholtz equation) by considering attenuation of sound wave in bulk liquid. The aim has been to predict the cavitational activity distribution using theoretical analysis and to compare the obtained results with experimentally obtained distribution.

Helmholtz equation has been solved by applying suitable boundary conditions as:

1. At the tip of transducer $P = P_0$ considering that the entire energy is entering into system through tip
2. At the wall $P = 0$, pressure amplitude vanishes near the wall

Table 2
Damping factor for NaCl solution.

Sr. No	Concentration of NaCl solution % (w/v)	Damping factor for 204 kHz (1/m)	Damping factor for 694 kHz (1/m)
1	0 (water)	3.28×10^{-4}	3.79×10^{-3}
2	1	3.32×10^{-4}	3.87×10^{-3}
3	5	3.60×10^{-4}	4.17×10^{-4}
4	10	3.99×10^{-4}	4.62×10^{-4}

For solution of the equations, acoustic module from COMSOL Multi-physics simulation tool (version 3.3) has been used which considers finite element method as numerical solution technique for the model consisting of set of ordinary differential equations.

2.5.1. Determination of damping factor

The intensity of sound wave decreases with an increase in the distance from irradiating surface due to attenuation. Attenuation mainly occurs due to the conversion of kinetic energy associated with the waves into heat. Moholkar et al. [12] have reported that attenuation coefficient is a function of physicochemical properties of the liquid medium, velocity of sound in the medium as well as operating frequency of ultrasound and can be estimated by the following equation:

$$\alpha_s = \frac{8\mu\pi^2 f^2}{3\rho c^3} \tag{3}$$

where μ is viscosity (kg/m s^2), f is frequency of ultrasound (Hz), ρ is density of liquid (kg/m^3), and c is speed of sound (m/s).

For the present system, the values of damping factor calculated for water and aqueous solution of NaCl have been reported in Table 2.

2.5.2. Determination of speed of sound wave in NaCl solution

Wilson [13] has proposed an empirical equation for predicting the speed of sound in the sea water. It has been considered that speed of sound is a function of density of water, amount of salt present that is salinity, temperature and hydrostatic pressure and can be given by following Eq. (2):

$$C(S,T,P) = C_0 + \Delta C_T + \Delta C_S + \Delta C_P + \Delta C_{STP} \tag{4}$$

where $C_0 = 1449.14$

$$\Delta C_T = 4.5721T - 4.453.2 \times 10^{-2}T^2 - 2.6045 \times 10^{-4}T^3 + 7.9851 \times 10^{-6}T^4$$

$$\Delta C_S = 1.39799 \times (S-35) - 1.69202 \times 10^{-3} \times (S-35)^2$$

$$\Delta C_P = 1.63432 \times P - 1.06768 \times 10^{-3} \times P^2 + 3.73403 \times 10^{-6} \times P^3 - 3.6332 \times 10^{-8} \times P^4$$

$$\begin{aligned}\Delta C_{STP} = {} & (S-35)[(-1.1244 \times 10^{-2} \times T) + (7.7711 \times 10^{-7} \times T^2) \\ & + (7.85344 \times 10^{-4} \times P) - (1.3458 \times 10^{-5} \times P^2) \\ & + (3.2203 \times 10^{-7}PT) + (1.6101 \times 10^{-8}T^2P)] \\ & P \times [(-1.8974 \times 10^{-3}T) + (7.6287 \times 10^{-5}T^2) \\ & + (4.6176 \times 10^{-7}T^3)] \\ & + P^2[(-2.6301 \times 10^{-5} \times T + 1.9302 \times 10^{-7}T^2) +] \\ & + P^3[(-2.0831 \times 10^{-7}T)]\end{aligned}$$

where $C(S, T, P)$ is speed of sound (m/s), T is liquid temperature (°C), S is salinity (per mille), and P is hydrostatic pressure (MPa).

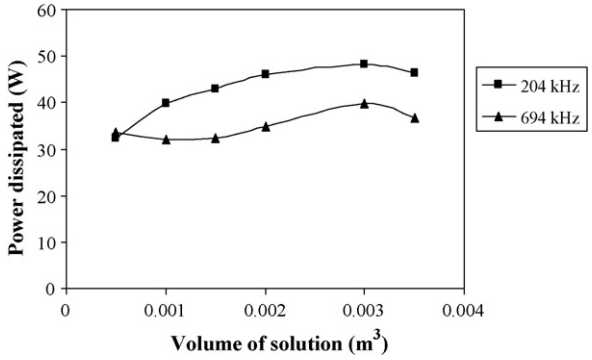

Fig. 2. Variation in calorimetric power dissipation in bulk liquid with operating capacity.

Wilson's formula is valid for the temperature range of −4 to 30 °C, salinity 0–37 per mille and hydrostatic pressure 0.1–100 MPa. In present case, all experiments were performed at atmospheric pressure and room temperature around 25 ± 1 °C. Applicability of above equation has been checked by estimating speed of sound in normal water (by considering density = 997, temperature = 28 °C and salinity = 0 and pressure = 1 atm) as 1496.8 m/s. As the density for NaCl solution increases, speed of sound also increases as 1503.1, 1507, 1513.54 m/s respectively for 1%, 5% and 10%. NaCl solution.

2.6. Bubble dynamics studies

For bubble dynamics analysis, Rayleigh–Plesset Noltingk Neppiras equation (which also considers the effects of the medium physicochemical properties) has been used to explain the cavity behavior under the influence of acoustic field and has been given as follows:

$$R\left(\frac{d^2R}{dt^2}\right) + \frac{3}{2}\left(\frac{dR}{dt}\right)^2 = \frac{1}{\rho_l}\left[P_i - \frac{4\mu}{R}\left(\frac{dR}{dt}\right) - \frac{2\sigma}{R} - P_\infty\right] \tag{5}$$

where P_i is the pressure inside the bubble at time t, R is the instantaneous cavity radius, μ is the viscosity of the liquid, σ is the surface tension of the liquid medium, and P_∞ is the driving local pressure field. This equation is a second-order nonlinear differential equation and has been solved numerically using the fourth-order Runge–Kutta–Nystrom method.

For single-frequency (f) operation, the local pressure field under the influence of acoustic field can be given by:

$$P_\infty = P_0 - P_A(\sin 2\pi ft) \tag{6}$$

where P_0 is the ambient pressure, P_A is the pressure amplitude due to the ultrasonic intensity of irradiation, given as:

$$P_A = \sqrt{2I\rho C} \tag{7}$$

where I is the intensity of ultrasound (W/m^2), ρ the density of the medium (kg/m^3) and C the velocity of sound in the medium (m/s).

3. Results and discussion

3.1. Power dissipation

Investigations related to quantification of calorimetric power dissipation were performed with varying capacity in pure water. The obtained results have been given in Fig. 2. It can be seen from the figure that as the reaction volume increases, power dissipation in bulk liquid increases up to an operating capacity of 3 l (with maximum power dissipated as 48.11 and 39.74 W respectively for 204 and 694 kHz frequencies) and then marginally decreases. An optimum operating volume of reactor has been selected as 3 l for

Table 3
Calorimetric power dissipation for 204 and 694 kHz frequencies at 3 l and for irradiation time of 10 min.

Sr. No.	Amount of NaCl solution % (w/v)	204 kHz	% Increase in power dissipation rate	694 kHz	% Increase in power dissipation rate
1	0 (water)	48.11	–	39.74	–
2	1	58.69	21.99	40.87	2.84
3	5	70.58	46.70	42.76	7.59
4	10	75.95	57.86	45.57	14.67

Table 4
Quantitative comparison for amount of iodine liberation in various planes.

Operating mode	Plane 1 (mg/l)	Plane 2 (mg/l)	Plane 3 (mg/l)	Plane 4 (mg/l)	Plane 5 (mg/l)	Total (mg/l)	Power* (J)	(Total iodine liberated)/power
204 kHz	19.84	8.92	16.91	18.22	13.28	65.18	9.41×10^5	6.92×10^{-5}
204 + 10%	38.51	31.43	26.64	35.89	24.82	157.30	1.39×10^6	1.113×10^{-4}
204 + 5%	28.12	19.90	12.6	22.07	14.79	97.48	1.21×10^6	8.12×10^{-5}
204 + 1%	22.88	10.91	17.24	19.42	11.89	82.35	1.05×10^6	7.84×10^{-5}
694 kHz	7.82	3.00	2.28	3.43	2.27	18.82	6.78×10^5	2.77×10^{-5}
694 +10%	9.21	4.07	3.04	5.45	5.00	26.79	8.66×10^5	3.09×10^{-5}
694 +5%	6.70	4.02	2.45	4.39	3.36	20.93	7.56×10^5	2.76×10^{-5}
694 +1%	7.54	3.44	2.92	3.97	2.50	20.38	1.03×10^6	1.97×10^{-5}

* Power dissipation is for irradiation time of 3 min.

both the frequencies. The calorimetric efficiency was 24% and 20.1% respectively for 204 and 694 kHz for the 3 l operating capacity.

At the capacity of 3 l, power dissipation was estimated in aqueous NaCl solutions. The concentration of NaCl solution was varied over a range 1–10% (by weight) for both frequencies. The obtained results have been given in Table 3. It can be seen from the data that the extent of power dissipation increases with an increase in the salt concentration and maximum power dissipation is obtained at 10% NaCl solution for both the frequencies. It can be seen that around 57.86% and 14.67% increase in power dissipation is observed in the presence of 10% (w/v) NaCl solution for 204 and 694 kHz frequency respectively.

3.2. Iodine liberation at various locations

In order to quantify active and passive zones in a reactor, studies with decomposition of potassium iodide have been carried out at different locations in various planes for both the operating frequencies in presence and absence of NaCl. The extent of decomposition of iodine at various planes (along vertical axis) for an operating frequency of 204 kHz in water has been shown in Fig. 3 as a representative plot. Similar distribution has been observed for the other frequencies and in absence/presence of NaCl solution. Quantification of the net iodine liberation in different planes for different operating conditions has been given in Table 4.

From Table 4, it can be observed that maximum cavitational activity was observed in plane 1 (19.84 mg/l, 2.16 cm from bottom) which is just above the irradiating surface. As we go away from irradiating surface (from plane 2 to 5) cavitational activity decreases up to plane 3 and marginal increase was obtained at plane 4 (18.22 mg/l, 3.14 cm from air–liquid interface) which can be attributed to the possible formation of interference of waves at this location. However it should be noted that, lower iodine liberation was observed in plane 5 (1 cm from air–liquid) and this is due to the fact that only small part of test solution was exposed to cavitation (only 2 ml of KI solution). Also for plane 1, high activity was observed at the center of reactor whereas for remaining planes low activity zones are located at the center of reactor. The obtained results were in agreement with the trends obtained by Trabelsi et al. [14], who have performed experiments to identify the active zones in high frequency (561 kHz with maximum power rating of 50 W) cylindrical reactor of diameter of 6.2 cm and maximum operating capacity of 300 cm^3 by electrochemical method. Identification of distribution in various planes viz. axial and radial direction indicated that low cavitational activity is obtained at the center of reactor along the radial direction.

Similar kind of cavitational activity distribution has been obtained for 694 kHz but with lower magnitude of net iodine liberation. Maximum liberation was obtained at plane 1 (7.82 mg/l) and for remaining planes the quantum in the range of 2.27–3.43 mg/l. The lower net iodine liberation was attributed to effects of frequency as well as power dissipation in the reactor. For operating frequency of 694 kHz, the net power dissipation was always lower as compared to 204 kHz which resulted in a decrease in the number of cavitational events and hence quantum of free radicals being available for release of iodine. Comparison in terms of iodine liberation per unit power also indicates higher efficacy of 204 kHz operating frequency as illustrated in Table 4. This variation in liberation with frequency mainly depends on the generation rate of free radicals and life time. For explaining the obtained dependency, bubble dynamics simulations have been performed for predicting the cavity lifetime as well as maximum radius reached by the growing bubble during the different phases of cavitation phenomena. The initial conditions for the simulations have been considered as 1 atm ambient pressure with initial cavity size of 2 μm, ambient temperature of 30 °C and dissolved gas fraction of 0.7. The obtained results have been given in Table 5. It can be seen from the table that with an increase in the frequency of irradiation, cavity collapse time decreases which results in lower extent of generation of free radicals and hence lower rates of iodine liberation. The numerical simulation results for effect of frequency matches closely with earlier theoretical results of Prabhu et al. [15]. The effect of frequency has also been investigated experimentally. Koda et al. [16] have performed experiments on Fricke, iodine dosimeter and decompo-

Table 5
Results of the cavity dynamics simulation.

Sr. No.	Operating mode	Cavity collapse time (μs)	R_{max}/R
1	204 kHz	3.43	6.22
2	204 + 1%	3.61	7.34
3	204 + 5%	3.78	8.39
4	204 + 10%	3.84	8.80
5	694 kHz	1.05	2.23
6	694 + 1%	1.06	2.27
7	694 + 5%	1.07	2.32
8	694 + 10%	1.09	2.40

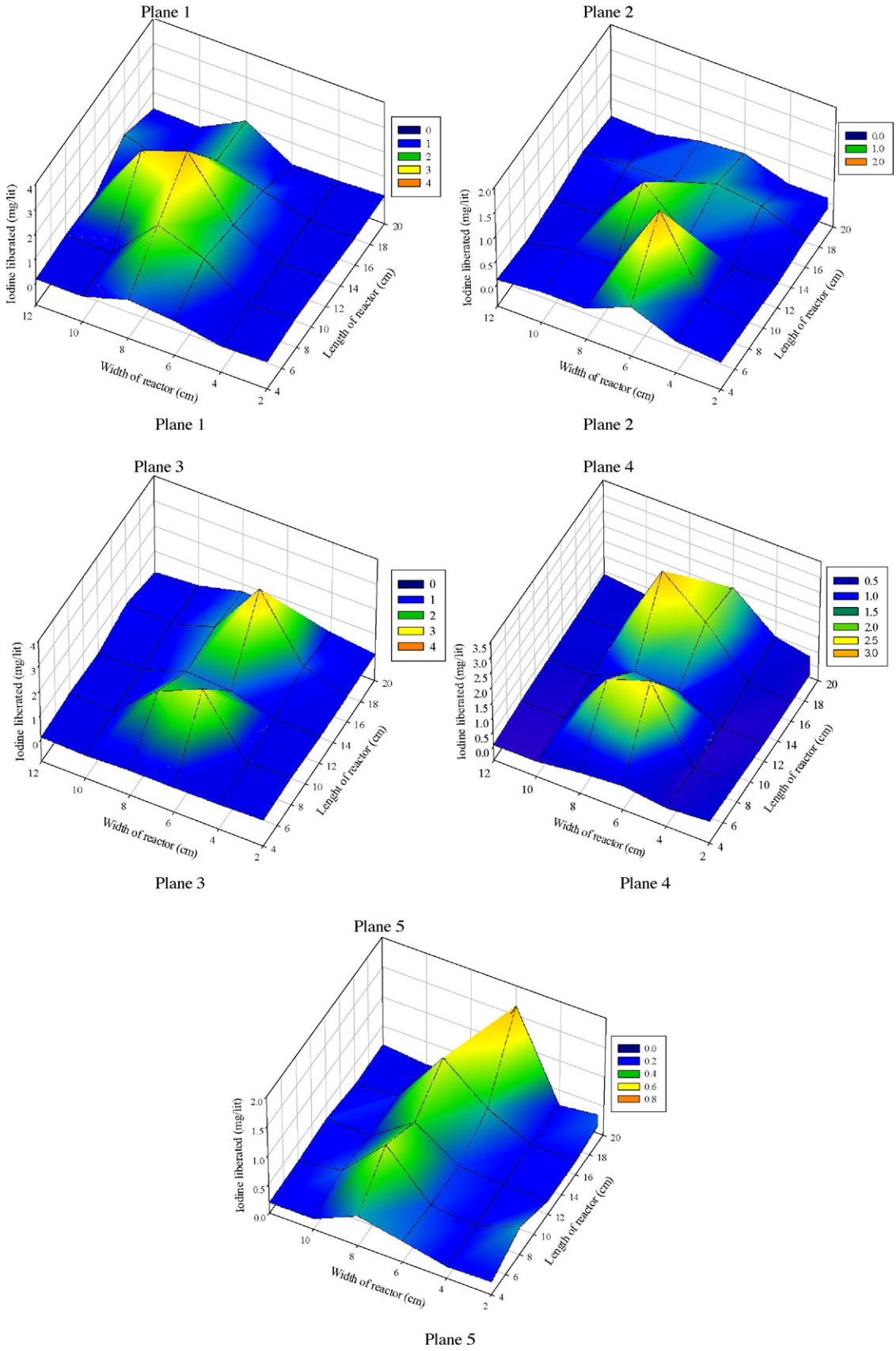

Fig. 3. Amount of iodine liberated in various planes for 204 kHz frequency of irradiation.

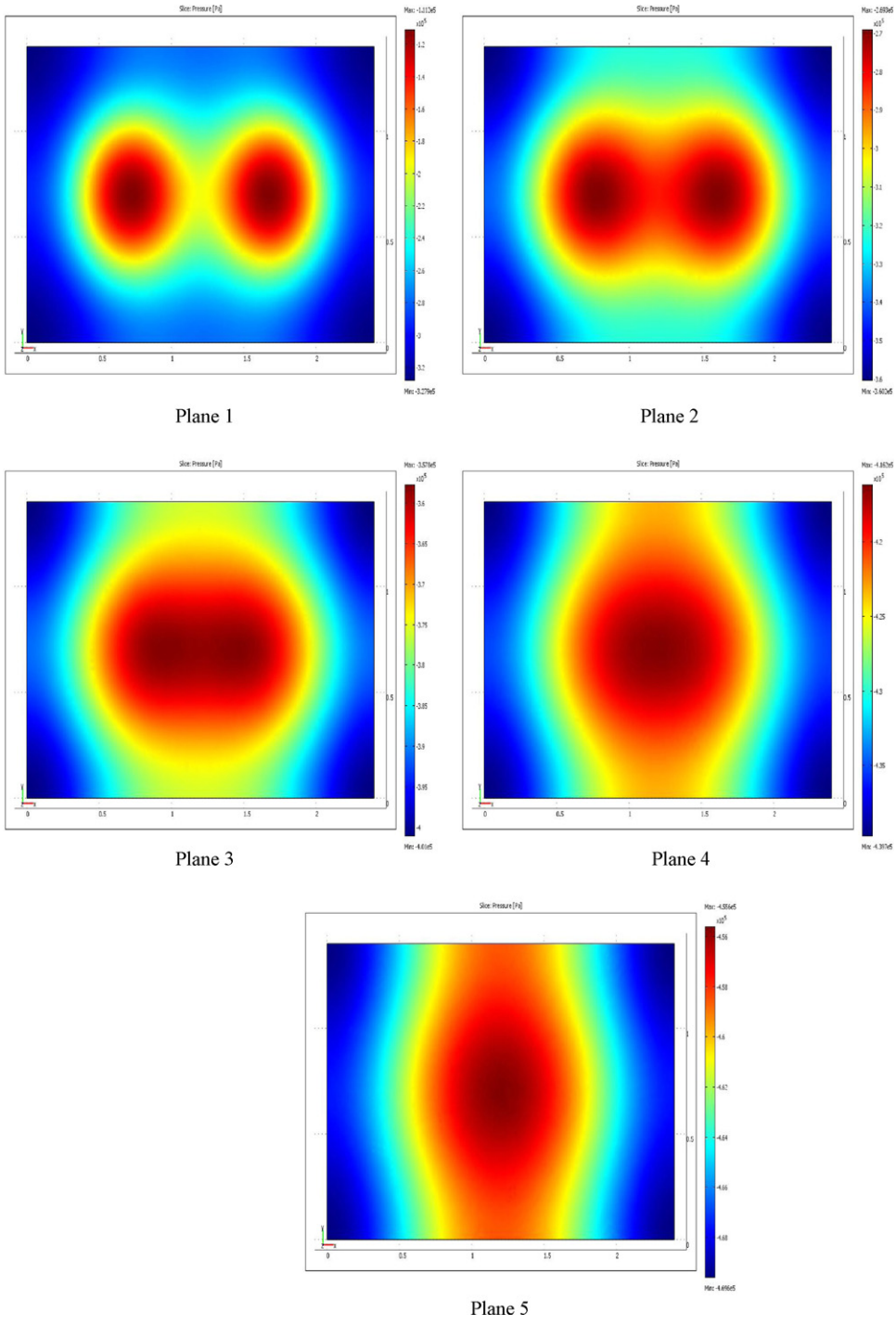

Fig. 4. Variation of cavitational activity distribution in reactor with 204 kHz frequency as predicted theoretically.

sition of porphyrin in the frequency range of 19.5 kHz to 1.2 MHz and conclude that there exists an optimum frequency at 300 kHz with maximum cavitational activity. Kang et al. [17] have reported that formation of hydrogen peroxide at higher frequencies of 618 and 1078 kHz is lower as compared to 300 kHz. Chand et al. [18] have performed degradation of phenol at three operating frequencies as 20, 300 and 520 and reported that maximum degradation was obtained at 300 kHz.

Comparison of the data obtained for different concentrations of NaCl solution (Table 4) indicates that the amount of iodine liberation is higher in the presence of NaCl and further it increases with an increase in the concentration of NaCl. Quantitatively the increase in total extent of iodine liberation (summation of liberation at all locations in a given plane) is about 140% higher for 10% salt solution as compared with only water. In order to check whether the enhancement was due to higher power dissipation rate or enhanced cavitational intensity due to the presence of NaCl in terms of collapse pressure or collapse temperature, the amount of iodine liberated per unit power dissipation for given interval of time has also been estimated as shown in Table 4. It can be seen that for 10% NaCl solution, higher liberation per unit power dissipated was obtained (1.113×10^{-4} (mg/l)/J) as compared to other concentrations indicating that both the effects are equally contributing. The results given in Table 5 for the numerical simulations also clearly

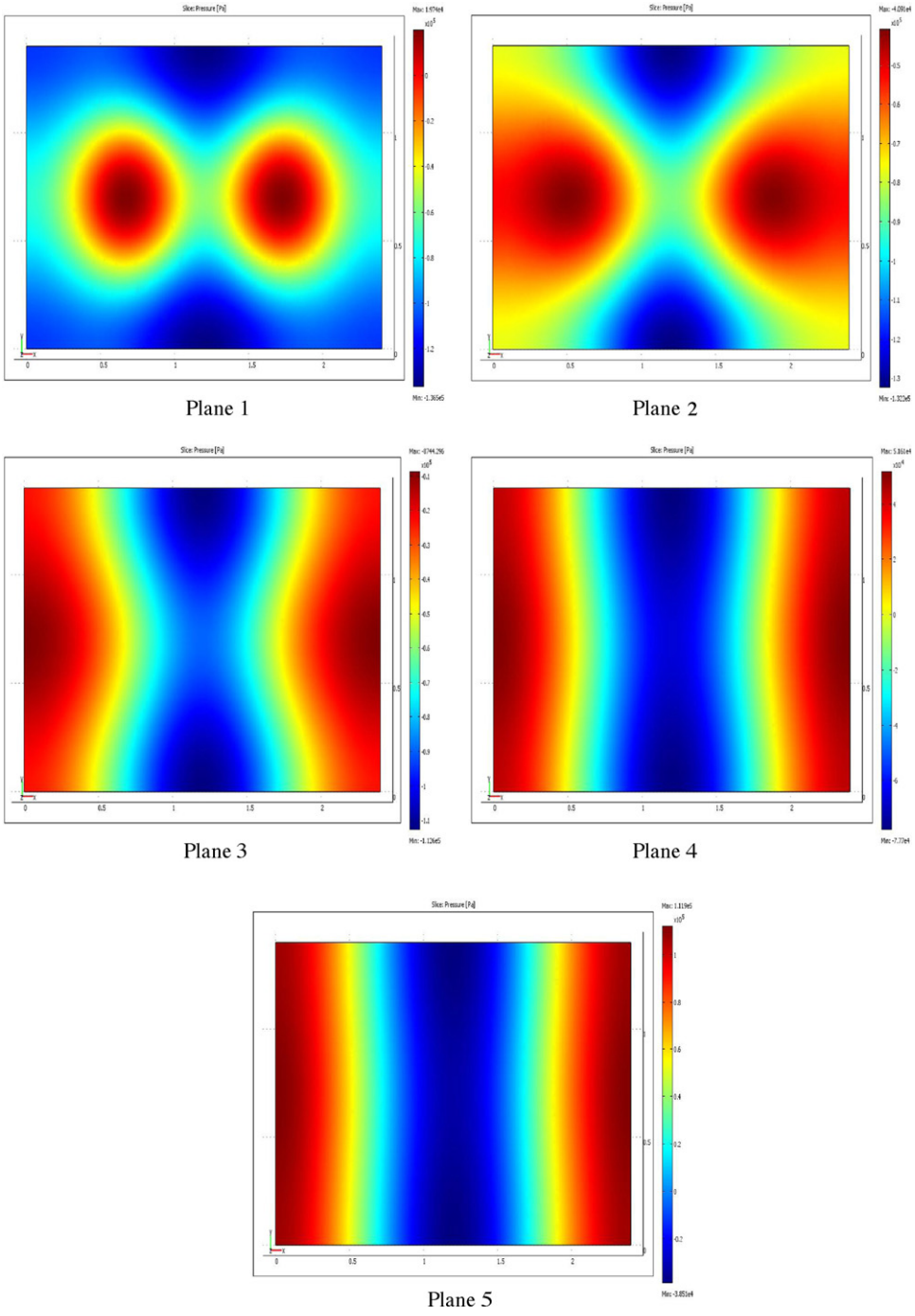

Fig. 5. Variation of cavitational activity distribution in reactor with 694 kHz frequency as predicted theoretically.

illustrate the higher cavitational intensity as indicated by higher growth of the generated cavity and quick collapse resulting in generation of higher extent of collapse pressure and temperature. As the size of cavity marginally increases (around 12%) with sufficient increase in cavity collapse time (42%), larger number of free radicals are generated and hence the extent of iodine liberation also increases.

3.3. Quantification of local pressure field by wave equation

Cavitational activity was estimated in sonochemical reactor at various planes for frequencies of irradiation of 204 and 694 kHz using NaCl solution and the obtained results are shown in Figs. 4 and 5 respectively. All simulations for water were performed at constant density of 997 kg/m^3, viscosity of 1 cP and speed of sound as 1496.8 m/s. Simulated geometry have 151,340 number of degree of freedom and 105,094 number of mesh elements.

It can be seen from figure that for both the operating frequencies, higher pressure amplitude is observed above the locations of the transducers and it decreases with an increase in the distance away from the transducer. It has been also observed that there exists some degree of cavitational activity over the entire region unlike conventional ultrasonic horn where the activity is concentrated very near to the transducer and exponentially decreases away from the transducers [5].

Table 6
Quantitative comparison of predicted pressure amplitude in various planes.

Operating mode	Plane 1 (atm)	Plane 2 (atm)	Plane 3 (atm)	Plane 4 (atm)	Plane 5 (atm)	Total (atm)	% Increase
204 kHz	2.19	3.14	3.79	4.37	4.62	18.11	–
204 + 10%	2.83	4.06	4.89	5.52	5.97	23.27	28.49
204 + 5%	2.62	3.78	4.56	5.15	5.58	21.69	19.76
204 + 1%	2.37	3.41	4.12	4.65	5.03	19.58	8.11
694 kHz	0.78	0.86	0.61	0.62	0.75	3.62	–
694 + 10%	0.93	1.1	0.71	0.81	0.92	4.47	23.48
694 + 5%	0.86	0.97	0.66	0.74	0.85	4.1	13.25
694 + 1%	0.81	0.92	0.63	0.69	0.79	3.84	6.07

Table 6 gives the cumulative pressure amplitude predicted using theoretical simulations over the entire plane. It can be seen from the table that the pressure amplitude in plane 1 very near to bottom of reactor is 2.19 atm and it increases towards plane 5 where it is maximum at 4.62 atm. In the case of 694 kHz frequency, maximum pressure amplitude was observed in plane 2 (0.86 atm) and for remaining planes variation was in the range of 0.61–0.78 atm. The predicted pressure amplitudes are higher for 204 kHz frequency as compared to 694 kHz frequency validating earlier discussion about the effects of frequency of irradiation.

In order to investigate the variation in pressure amplitude in the presence of NaCl solution, the calculated physicochemical properties have been used and simulations were performed. Similar kinds of results were obtained for the distribution of active and passive zones but with enhanced pressure amplitude. Quantitative comparison for the obtained pressure amplitude has been depicted in Table 6.

In order to correlate the primary effects (simulated pressure amplitude) with secondary effects (decomposition of KI) comparison of the obtained results in different planes for iodine liberation and cumulative pressure amplitude has been made. It has been observed that the initially iodine liberation was found to increase with an increase in pressure amplitude up to 3.25 atm and then decrease with further increase in the pressure. Also it should be noted that minimum threshold pressure required to commence the iodine liberation is 0.61 atm. This existence of threshold pressure can be attributed due to the fact that certain minimum numbers of free radicals are required to initiate iodine liberation.

Sravan et al. [19] have reported the measurement of pressure field distribution at various locations in a sonochemical reactor of operating capacity as 5.6 l and irradiating frequency of 45 kHz with maximum power rating as 230 W, with the help of hydrophone coupled with high speed data acquisition system. They have correlated the obtained pressure with chemical effects generated by decomposition of KI and reported similar existence of optimum and threshold pressure values. The obtained results have been attributed to the number and size of bubbles formed and it has been reported that at high pressure very high number of bubbles are formed but with smaller size that ultimately cause less violent collapse and hence low cavitational activity.

4. Conclusions

The distribution of cavitational activity in terms of iodine liberation in sonochemical reactor is non-uniform in nature. The current work of mapping in a pilot scale high frequency reactor has enabled us to identify the distribution in the reactor and establish the effectiveness as compared to a conventional horn type reactor. In general, the cavitational activity decreases with an increase in the distance from transducer though a marginal increase can be obtained due to interference of the incident and reflected waves from the liquid interface. Operating frequency of 204 kHz has been found to give more intense cavitational activity as quantified by higher extents of iodine liberation as well as predicted pressure amplitudes. The role of power dissipation as well as frequency of irradiation has been elucidated using bubble dynamics simulations. The presence of NaCl results in enhanced cavitational activity attributed to the change in physicochemical properties, leading to lower attenuation of sound waves and higher cavitational intensity as confirmed using theoretical simulations and also quantified in terms of the yields of iodine liberation. The present work has clearly established the role of power dissipation, frequency and presence of salts in intensifying the cavitational activity in the reactor.

Acknowledgement

PRG would like to acknowledge the funding of the Department of Science and Technology, New Delhi, India under the Hungarian – Indian Intergovernmental S&T Cooperation Programme.

References

[1] P.R. Gogate, Cavitational reactors for process intensification of chemical processing applications: a critical review, Chem. Eng. Proc. 47 (2008) 515.
[2] P.R. Gogate, A.M. Kabadi, A review of applications of cavitation in biochemical engineering/biotechnology, Biochem. Eng. J. 44 (2009) 60.
[3] L.H. Thompson, L.K. Doraiswamy, Sonochemistry: science and engineering, Ind. Eng. Chem. Res. 38 (1999) 1215.
[4] T.J. Mason, J.P. Lorimer, Applied Sonochemistry: The Uses of Power Ultrasound in Chemistry and Processing, Wiley-VCH Verlag GmbH, Weinheim, 2002.
[5] P.R. Gogate, P.A. Tatake, P.M. Kanthale, A.B. Pandit, Mapping of sonochemical reactors: review, analysis and experimental verification, AIChE J. 48 (2002) 1542.
[6] P.M. Kanthale, P.R. Gogate, A.B. Pandit, A.M. Wilhelm, Mapping of an ultrasonic horn: link primary and secondary effects of ultrasound, Ultrason. Sonochem. 10 (2003) 331.
[7] J. Seymour, R.B. Gupta, Oxidation of aqueous pollutants using ultrasound: salt induced enhancement, Ind. Eng. Chem. Res. 36 (1997) 3453.
[8] C.A. Wakeford, R. Blackburn, P.D. Lickiss, Effect of ionic strength on the acoustic generation of nitrite, nitrate and hydrogen peroxide, Ultrason. Sonochem. 6 (1999) 141.
[9] P.R. Gogate, I.Z. Shirgaonkar, M. Sivakumar, P. Senthilkumar, N.P. Vichare, A.B. Pandit, Cavitation reactors: efficiency assessment using a model reaction, AIChE J. 47 (2001) 2526.
[10] T. Kimura, T. Sakamoto, J.-M. Leveque, H. Sohmiya, M. Fujita, S. Ikeda, T. Ando, Standardization of ultrasonic power for sonochemical reaction, Ultrason. Sonochem. 3 (1996) S157.
[11] D.M. Kirpalani, K.J. McQuinn, Experimental quantification of cavitation yield revisited: focus on high frequency ultrasound reactors, Ultrason. Sonochem. 13 (2006) 1.
[12] V.S. Moholkar, S. Sabale, A.B. Pandit, Mapping the cavitational intensity in an ultrasonic bath using acoustic emission, AIChE J. 46 (2000) 684.
[13] W.D. Wilson, Equation for the speed of sound in sea water, J. Acoust. Soc. Am. 32 (1960) 1357.
[14] F. Trabelsi, H. Ait-Iyazidi, J. Berlan, P.-L. Fabre, H. Delmas, A.M. Wilhelm, Electrochemical determination of the active zones in a high-frequency ultrasonic reactor, Ultrason. Sonochem. 3 (1996) S125.
[15] A.V. Prabhu, P.R. Gogate, A.B. Pandit, Optimisation of multi frequency sonochemical reactors, Chem. Eng. Sci. 59 (2004) 4991.

[16] S. Koda, T. Kimura, T. Kondo, H. Mitome, A standard method to calibrate sonochemical efficiency of an individual reaction system, Ultrason. Sonochem. 10 (2003) 149.
[17] J.-W. Kang, H.-M. Hung, A. Lin, M.R. Hoffmann, Sonolytic destruction of methyl tert-butyl ether by ultrasonic irradiation: the role of O_3, H_2O_2, frequency, and power density, Environ. Sci. Technol. 33 (1999) 3199.
[18] R. Chand, N.H. Ince, P.R. Gogate, D.H. Bremner, Phenol degradation using 20, 300 and 520 kHz ultrasonic reactors with hydrogen peroxide, ozone and zero valent metals, Sep. Purif. Technol. 67 (2009) 103.
[19] K.S. Sravan, A. Balasubramanyam, S.P. Shyam, P.R. Gogate, V.D. Deshpande, S.R. Shukla, A.B. Pandit, Characterization of sonochemical reactor for physicochemical transformations, Ind. Eng. Chem. Res. 48 (2009) 9402.